Synthesis and Evaluation of Novel Polyaminocarboxylate-Based Antitumor Agents

Hyun-Soon Chong,* Xiang Ma, Haisung Lee, Phuong Bui, Hyun A. Song, and Noah Birch

Chemistry Division, Biological, Chemical, and Physical Sciences Department, Illinois Institute of Technology, Chicago, Illinois

Received October 17, 2007

Iron depletion, using iron chelators targeting transferrin receptor (TfR) and ribonucleotide reductase (RR), is proven to be effective in the treatment of cancer. We synthesized and evaluated novel polyaminocarboxylate-based chelators NETA, NE3TA, and NE3TA-Bn and their bifunctional versions C-NETA, C-NE3TA, and N-NE3TA for use in iron depletion tumor therapy. The cytotoxic activities of the novel polyaminocarboxylates were evaluated in the HeLa and HT29 colon cancer cell lines and compared to the clinically available iron depletion agent DFO and the frequently explored polyaminocarboxylate DTPA. All new chelators except C-NETA displayed enhanced cytotoxicities in both HeLa and HT29 cancer cells compared to DFO and DTPA. Incorporation of the nitro functional unit for conjugation to a targeting moiety into the two potent non-functionalized chelators NE3TA and NE3TA-Bn (C-NE3TA and N-NE3TA) was well-tolerated and resulted in a minimal decrease in cytotoxicity. Cellular uptake of C-NE3TA, examined using a confocal microscope, indicates that the chelator is taken up into HT29 cancer cells.

Introduction

Iron is a critical element for the function of the human body such as DNA synthesis and regulation of cell cycling.[1] However, free iron, if present in excess, can be dangerous, because it participates in the Haber−Weiss reaction wherein highly reactive oxygen species (ROS[a])[2] are generated causing life-threatening damage to tissues such as iron overloading diseases and cancers.[3] Many studies indicate that a high level of iron accumulated in animals and humans is associated with both the initiation and the progression of cancers.[4,5] It is known that cancer cells require more iron than normal cells and are sensitive to iron depletion.[6] The high demand of iron results from enhanced production of an iron storage protein, ferritin or transferrin receptor (TfR), which governs the uptake of iron into cells from transferrin (Tf).[7] The requirement of iron in cancerous cells is also enhanced because iron plays an essential role in the catalytic activity of iron-containing enzyme ribonucleotide reductase (RR). Two dimeric proteins (R1, R2) in RR catalyze the reduction of ribonucleotides to deoxyribonucleotides, the building blocks for DNA synthesis and repair.[6] Cancer cells including HeLa and colon cancers and colorectal liver metastates are found to overexpress TfR, RR, or other proteins involved in intracellular iron uptake.[8–11]

The enhanced requirement of iron in cancer cells as compared to normal cells makes iron depletion using iron chelators targeting TfR, RR, or other proteins involved in iron uptake one of the most efficient strategies to prevent or suppress the rapid proliferation of cancerous cells.[12–14] Iron chelators are reported to cause cellular iron depletion and exhibit potent cytotoxic activities on diverse cancer cells. Triapine (3-aminopyridine-2-carboxaldehyde thiosemicarbazones, Figure 1), a potent RR inhibitor is a promising iron depleting anticancer agent. Cell culture experiments conducted on epithelial ovarian cancer cells indicate that Triapine induces apoptosis through an intrinsic pathway.[15] Triapine has been administered intravenously in a number of phase I and II clinical trials involving patients of various cancers.[16] Hydrophilic iron chelators such as desferoxamine (DFO) and diethylene triamine pentaacetic acid (DTPA, Figure 1) have been extensively explored for iron depletion antitumor therapy. DFO was approved for treatment of iron overload diseases. In addition to its proven iron clearing efficacy, DFO was shown to be effective in inducing apoptotic cell death and exhibited inhibitory and antiproliferative activity on tumor cells, including leukemia, bladder carcinoma, and hepatocelluar carcinoma, most likely due to RR inhibition as a consequence of iron depletion.[17–19] Two clinical trials involving leukemia patients resulted in the reduction of peripheral blast cell counts, purportedly suggesting significant potential of DFO as an antileukemic agent.[20,21] Polyaminocarboxylate chelator DTPA is an extracellular iron depletion agent.[22] Antitumor inhibitory activity of DTPA was demonstrated using human neuroblastoma[23] and ovarian carcinoma cell lines.[24] DTPA displayed iron mobilizing capability comparable to DFO in the clinical study of the iron-overloaded thalassaemic patients.[25]

Our research has been focused on development of potent iron chelators for iron depletion antitumor therapy.[12,13] As an ongoing effort, we have investigated novel polyaminocarboxylate chelators as antitumor agents. Herein, we report the synthesis and evaluation of the new polyaminocarboxylates NETA, NE3TA, and NE3TA-Bn and their bifunctional versions *C*-NETA, *C*-NE3TA, and *N*-NE3TA (Figure 2). Cytotoxicity of the new chelators was measured in the HeLa and HT29 cancer cells and compared to that of the clinically used iron chelators DFO and DTPA. A potent bifunctional ligand *C*-NE3TA containing a fluorescent moiety NBD (Figure 2) was synthesized and evaluated for cellular uptake of the chelator.

Results and Discussion

The structures of the novel chelators NETA,[26] NE3TA, NE3TA-Bn, *C*-NETA,[27a] *C*-NE3TA,[27b] and *N*-NE3TA that have been developed in our laboratory and evaluated in the present study are shown in Figure 2. Previous reports on iron depletion capability of DTPA prompt us to explore the new polyaminocarboxylate chelators as antitumor agents. Because NETA possesses the same coordinating groups to DTPA, we wanted to investigate NETA as an iron chelator using HeLa cells which

* To whom correspondence should be addressed. Tel.: 312-567-3235. Fax: 312-567-3494. E-mail: chong@iit.edu.

[a] Abbreviations: ROS, reactive oxygen species; Tf, trasferrin; TfR, transferrin receptor; RR, ribonucleotide reductase; IDT, iron depletion therapy; DFO, desferoxamine, DTPA, diethylene triamine pentaacetic acid.

10.1021/jm701307j CCC: $40.75
Published on Web 03/18/2008

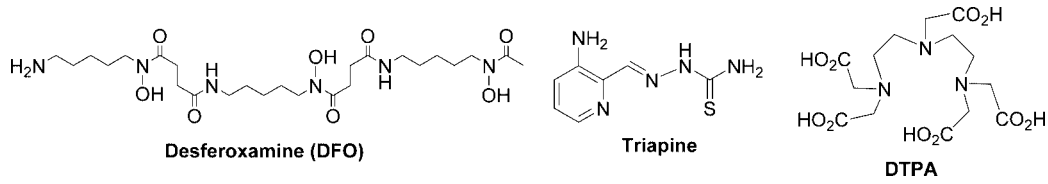

Figure 1. Iron chelators for antitumor therapy in clinical use.

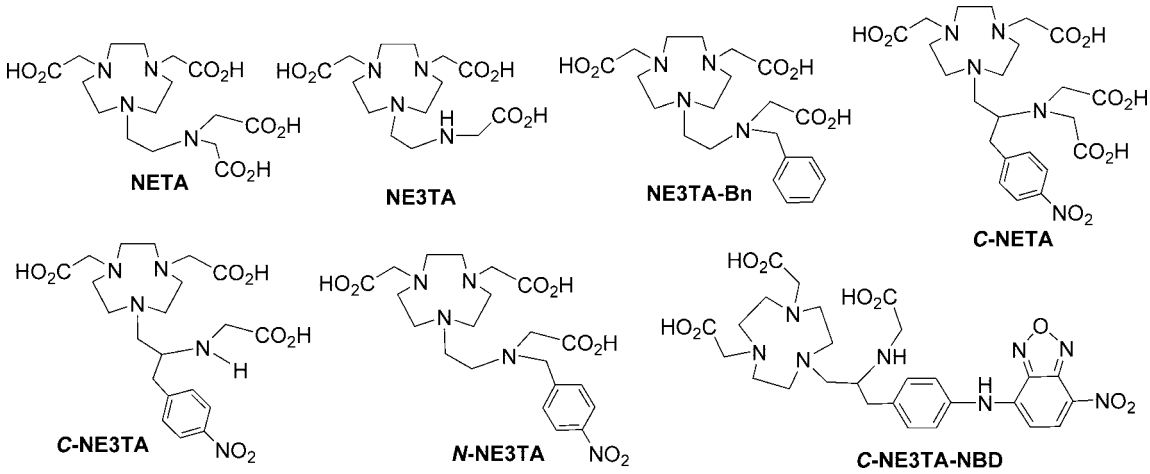

Figure 2. Novel polyaminocarboxylate-based antitumor conjugates.

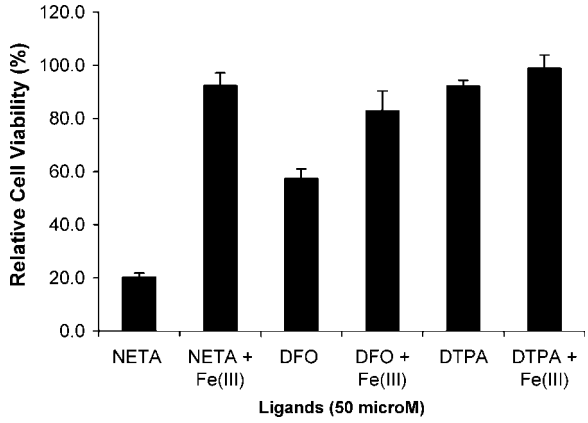

Figure 3. Effects of iron saturation and chelators on HeLa cell growth.

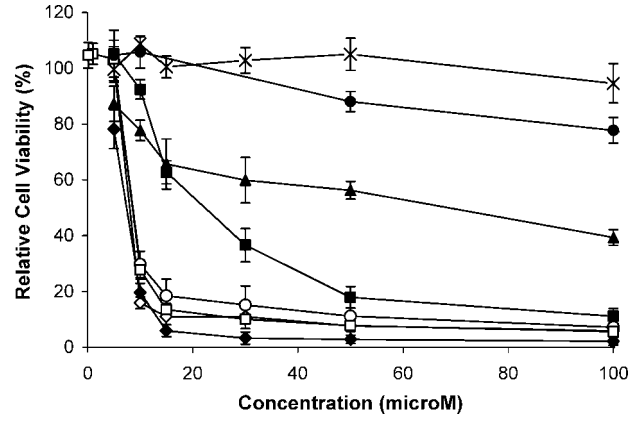

Figure 4. Effects of chelators DFO (▲), DTPA (●), NETA (■), NE3TA (◊), C-NETA (×), N-NE3TA (□), NE3TA-Bn (♦), and C-NE3TA (○) on viability of HeLa cancer cells.

are known to overexpress TfR. Octadentate NETA possesses both macrocyclic and acyclic moiety and is proposed to form a stable complex with a metal with fast complexation kinetics based on bimodal binding approach using both moieties.[26] The preliminary cell culture experiments were performed to see if NETA is an effective cytotoxic agent. As shown in Figure 3, NETA (50 μM) proliferated. NETA also displayed a 3-fold increased antiproliferative activity compared to DFO (Figure 3). To investigate the effect of the chelators on the cellular growth, the HeLa cancer cells were incubated with Fe(III)−citrate (50 μM) saturated with each of the chelators (50 μM). Inspection of Figure 3 indicates that almost no antiproliferative activity was observed with NETA and DTPA, while DFO resulted in a modest increase in cell viability as compared to nonsaturated cancer cells. The result suggests that the antiproliferative activity of NETA may result from iron chelation. Cytotoxicity of NETA in a series of concentrations was evaluated using the HeLa cell line and compared to the clinically available DFO and DTPA (Figure 4).[10] NETA exhibited significantly enhanced cytotoxicity, while DTPA resulted in almost no cytotoxicity in the HeLa cells. NETA and DTPA possess the respective IC_{50} of 30.8 ± 4.0 and 264.5 ± 36.2 μM (Table 1). Cytotoxicity of DFO is not concentration-dependent and was much lower than that of NETA.

Table 1. IC_{50} Values of Chelators in HeLa and HT29 Cancer Cells[a]

	IC_{50} (μM)	
ligand	HeLa	HT29
NETA	30.8 ± 4.0	7.3 ± 1.5
NE3TA	5.7 ± 0.3	4.7 ± 0.3
NE3TA-Bn	4.4 ± 0.9	2.6 ± 0.2
C-NETA	>100	45.7 ± 4.0
C-NE3TA	7.1 ± 0.1	5.0 ± 0.7
N-NE3TA	8.4 ± 0.4	6.8 ± 0.4
DFO	>50	36.1 ± 1.4
DTPA	264.5 ± 36.2	39.1 ± 4.0

[a] The chelators were incubated with the cells for 72 hrs, and the cell viability was determined using MTS assay.

With the promising cytotoxicity data of NETA, we wanted to evaluate a NETA analogue, NE3TA, which possesses seven

Scheme 1. Synthesis of Nonfunctionalized Ligand NE3TA

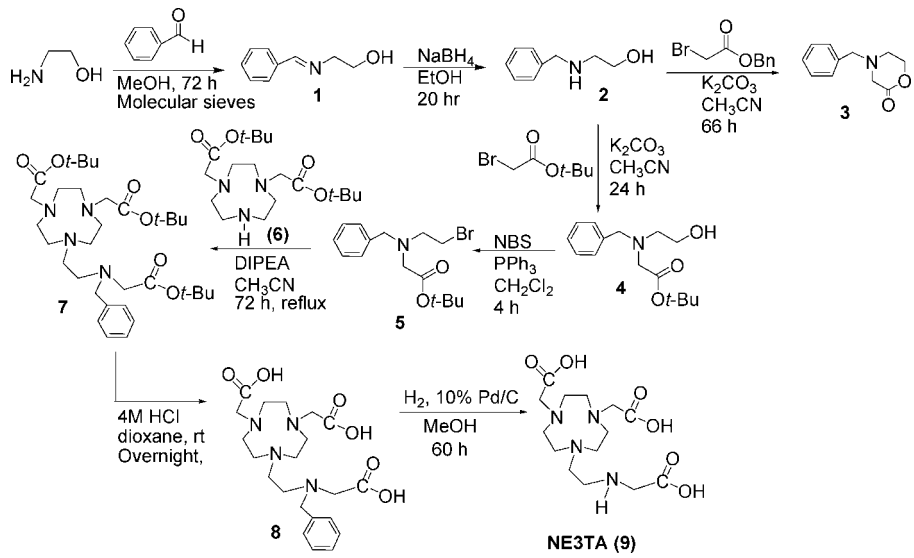

coordinating groups, that may be more effective in binding to the hexacoordinate iron than eight coordination groups in NETA. An efficient and short method to prepare NE3TA is shown in Scheme 1. The key step is the coupling reaction of macrocyclic and acyclic backbones, that is, *N*-Bn-protected monoalkylated bromide **5** and bisubstituted tacn derivative **6**[28] in a ratio of 1:1. Compound **5** was prepared starting from the readily available ethanol amine. Reaction of ethanol amine with benzaldehyde and further reductive amination provided *N*-benzyl ethanol amine **2**.[29] Initially, we attempted the alkylation reaction of **2** with benzyl bromoacetate. However, the reaction provided intramolecular rearrangement product morpholinone **3**, which was confirmed by both ^{1}H and ^{13}C NMR and HRMS. Reaction of **2** with *t*-butyl bromoacetate provided the alkylated product **4**, which was then further converted to bromide **5**. The reaction of **5** and **6** successfully provided **7** in good yield (71%). Isolation of the polar and tailing compound **7**, which can be monitored by HPLC and TLC analysis due to the presence of a benzylic UV chromophore was achieved by simple flash column chromatography eluting with 5–6% CH_3OH/CH_2Cl_2. *t*-Butyl groups in **7** were removed by 4 M HCl to provide NE3TA-Bn (**8**), which was subjected to hydrogenation to remove the benzyl protecting group, thereby affording the desired chelator NE3TA (**9**). NE3TA and NE3TA-Bn were evaluated for cytotoxicity using the HeLa cells (Figure 4). Among all nonfunctionalized ligands, NE3TA-Bn displays the highest activity against HeLa cells. Replacement of hydrogen in NE3TA by a benzyl group resulted in a slight increase in cytotoxicity. It seems that the presence of lipophilic benzyl group in NE3TA-Bn may result in some increase in cellular permeation, thus leading to enhanced cytotoxicity. NE3TA and NE3TA-Bn possessing the respective IC_{50} of 5.7 ± 0.3 and 4.4 ± 0.9 (Table 1) NE3TA-Bn, and NE3TA-Bn were further evaluated for cytotoxicity in the HT29 cancer cells (Figure 5) and compared to NETA, DTPA, and DFO. NE3TA and NE3TA-Bn produce higher antiproliferative activity in HT29 cells with the respective IC_{50} value of 4.7 ± 0.3 and 2.6 ± 0.2 (Table 1) than other chelators evaluated. All chelators tested produced enhanced activity in HT29 cancer cells compared to the HeLa cells (Figures 4 and 5). NETA possesses significantly decreased IC_{50} value in HT29 cells compared to the HeLa cells (7.3 ± 1.5 vs 30.8 ± 4.0, Table 1).

The result prompted us to evaluate a bifunctional version of NETA, NE3TA, and NE3TA-Bn that can be employed for targeted iron depletion therapy (IDT) by conjugation of the bifunctional iron chelator to a tumor targeting moiety such as antibody or peptide. The structure of bifunctional chelators, *C*-NETA,[27a] *C*-NE3TA,[27b] and *N*-NE3TA is shown in Figure 2. The bifunctional ligands possess a nitro group which can be further converted to an amino (NH_2) or isothiocyanate (NCS) group for conjugation to a tumor targeting peptide or antibody. *N*-functionalized NE3TA (*N*-NE3TA) was prepared based on the synthetic strategy involving the key coupling reaction that was used for the preparation of NE3TA. The starting material, *p*-nitrobenzaldehyde was reacted with amino ethanol to provide imine which was further reduced to *N*-(*p*-nitrobenzyl)ethanol amine **10**.[30] Reaction of **10** with *t*-butyl bromoacetate and subsequent bromination provided the precursor molecule **12** for the coupling reaction. Reaction of bisubstituted tacn **6** with **12** provided the desired product **13**. Treatment of *t*-butyl groups in **13** with 4 M HCl afforded the desired ligand *N*-NE3TA **14** (Scheme 2).

The cytotoxicity of the bifucntional ligands *C*-NETA, *C*-NE3TA, and *N*-NE3TA was evaluated using the HeLa and HT29 cell lines. Inspection of the data in Figures 4 and 5 indicates that introduction of a functional unit, *p*-nitro-benzyl group into NE3TA backbone via carbon substitution (*C*-NE3TA)

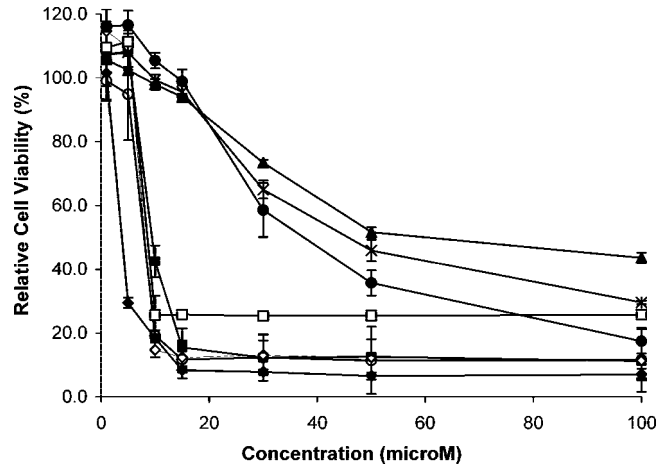

Figure 5. Effects of chelators DFO (▲), DTPA (●), NETA (■), NE3TA (◇), C-NETA (×), N-NE3TA (□), NE3TA-Bn (♦), and C-NE3TA (○) on viability of HT29 cancer cells.

Scheme 2. Synthesis of *N*-Functionalized Ligand *N*-NE3TA

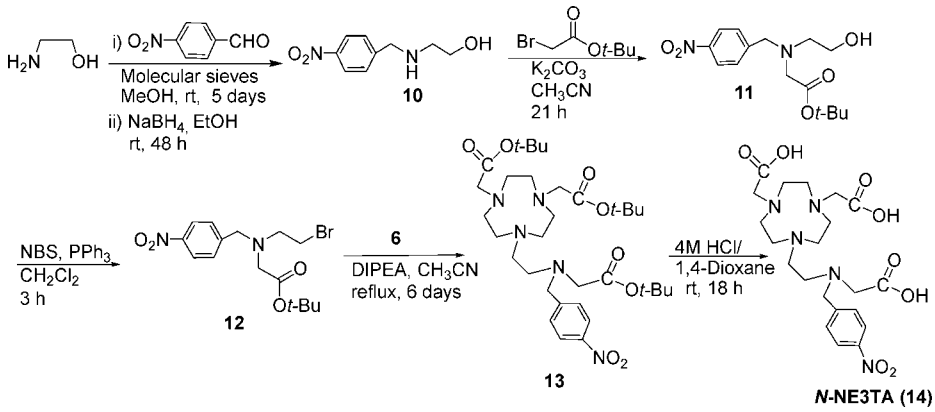

Scheme 3. Synthesis of Fluorescent Antitumor Agent *C*-NE3TA-NBD

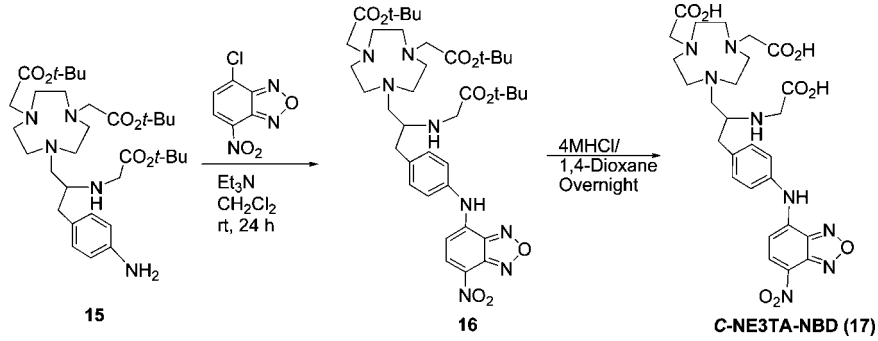

or nitrogen substitution (*N*-NE3TA) is well-tolerated and resulted in minimal decrease in cytotoxicity as compared with NE3TA. IC_{50} value of 7.1 ± 0.1 μM and 8.4 ± 0.4 μM using the HeLa cells was observed with *C*-NE3TA and *N*-NE3TA, respectively. Both compounds displayed a slight increase in IC_{50} value in HT29 cells (5.0 ± 0.7 μM and 6.8 ± 0.4 μM for *C*-NE3TA and *N*-NE3TA, respectively) as compared to the HeLa cells. However, *C*-functionalized NETA (*C*-NETA) displayed virtually no inhibitory activity against the HeLa cells over all the entire concentration range evaluated (Figure 4), while the antiproliferative activity of *C*-NETA (IC_{50} = 45.7 ± 4.0 μM), which is similar to that of DFO and DTPA was observed with HT29 cells (Figure 5).

The cytotoxicity of the chelators (50 μM) in the cancer cells was compared to their cytotoxicities in noncancer cells using human lung fibroblast cell line (MRC-5). The data shown in Figure 6 indicate that when the normal cells were treated with DFO, there was almost no change in cell viability as compared to that of the HeLa and HT29 cancer cells. No differential cytotoxicity between the cancer cells and the normal cells was observed with DFO. A 2-fold lowered cytotoxicity of normal cells compared to HT29 cancer cells was observed with DTPA, while there was no difference in cytotoxicity between HeLa cancer cells and normal cells treated with the chelator. All new chelators except for *C*-NETA displayed about 2∼8 times enhanced proliferative activity in normal cells as compared to the HeLa and HT29 cancer cells. The data indicate that the rapidly proliferating cancer cells were more effectively inhibited by all of the new polyaminocarboxylate chelators than normal

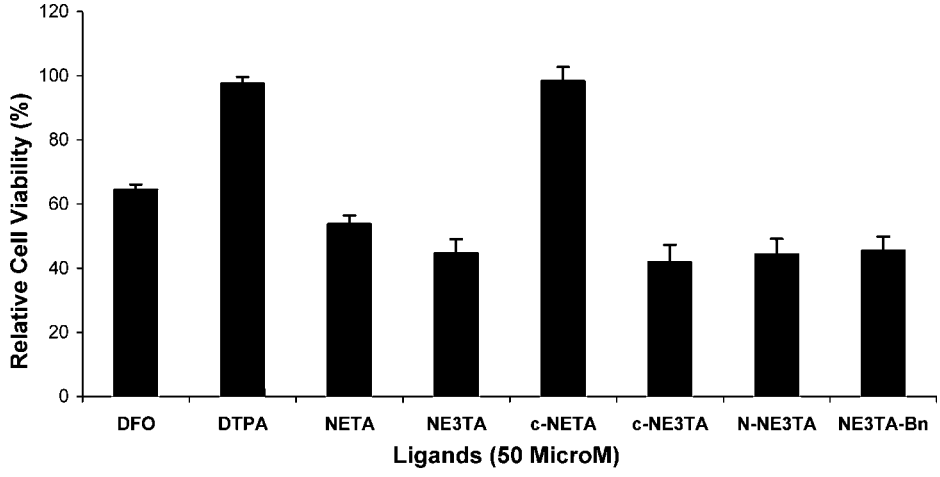

Figure 6. Antiproliferative activity of ligands against MRC-5 cells.

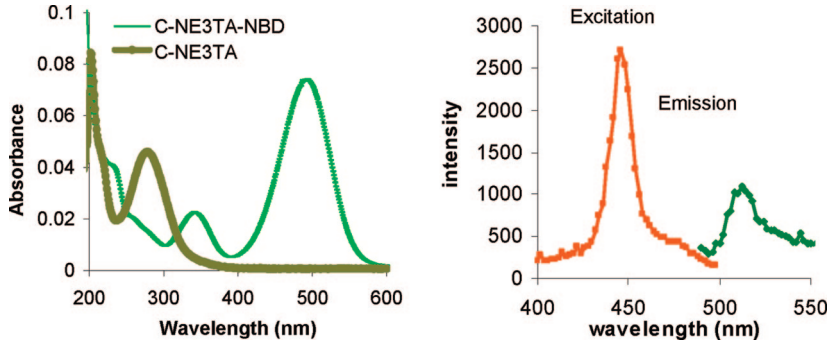

Figure 7. UV and fluorescence spectra of C-NE3TA and *C*-NE3TA-NBD (10 μM, H_2O).

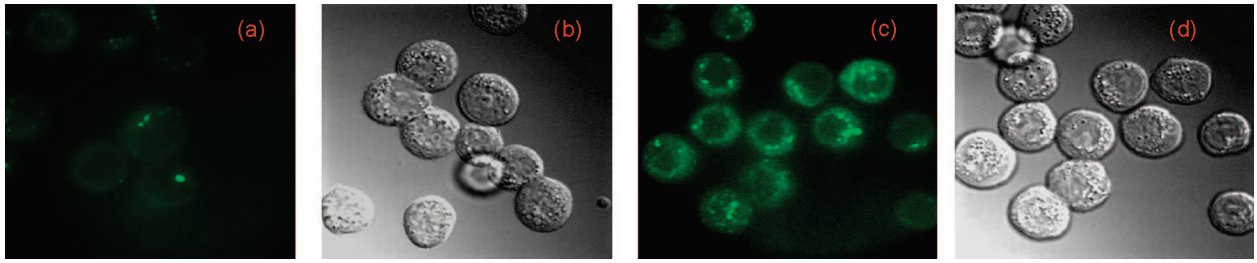

Figure 8. Fluorescence images of HT29 cancer cells; (a,b) control cancer cells; (c,d) the cells incubated with *C*-NE3TA-NBD (50 μM, H_2O) for 30 min at 37 °C; (b,d) phase contrast images.

cells, supporting the proposed hypothesis that cancer cells require more iron than normal healthy cells.

To visualize cellular uptake using fluorescence imaging, *C*-NE3TA was conjugated with an organic fluorescent moiety, NBD, to produce *C*-NE3TA-NBD (Scheme 3). Thus, the starting material **15**[27b] was reacted with NBD-Cl to provide the fluorescent conjugate **16**. *t*-Butyl groups in **16** were removed by treating 4 M HCl in 1,4-dioxane. UV and fluorescence spectra of *C*-NE3TA-NBD are shown in Figure 7. C-NE3TA-NBD has the respective excitation and emission wavelength of 446 and 512 nm. Fluorescence and phase contrast images of control HT29 cells or HT29 cells incubated with *C*-NE3TA-NBD (50 μM) were obtained using a confocal microscope with a band-pass filter set at 436/20nm (excitation) and 535/30nm (emission). Fluorescence images shown in Figure 8 indicate that C-NE3TA-NBD does accumulate in the HT29 cancer cells. It was noted that the control HT29 colon cancer cells also emit autofluorescence at the wavelength of excitation, as shown in Figure 8. While polyaminocarboxylate NE3TA is too hydrophilic to enter the cancer cells, *C*-NE3TA-NBD containing liphophilic moieties, both benzyl and NBD groups, is proposed to penetrate into the cells, resulting in the punctuate green fluorescence appeared in the cancer cells.

The cytotoxicity data indicate that the novel nonfunctionalized polyamine-carboxylates display significantly enhanced inhibitory activity against the HeLa and HT29 cancer cells as compared to the clinically available iron depletion agent DFO. Introduction of a bifunctional unit (*p*-nitrobenzyl) to the NE3TA backbone (*C*-NE3TA and *N*-NE3TA) was achieved without compromising the cytotoxic activity of NE3TA. *C*-NE3TA conjugated with NBD was taken up into HT29 cancer cells.

Conclusion

We have prepared the novel polyaminocarboxylates and evaluated their cytotoxicities using the HeLa and HT29 cancer cell lines. The polyaminocarboxylate chelators NETA, NE3TA, and NE3TA-Bn were found to display antiproliferative activity, which is much greater than the clinically available agents DFO and DTPA in both cancer cells. The promising antitumor polyaminocarboxylate-based chelators were functionalized via introduction of a nitro group, which can be further modified to either an amino or a isothiocyanate group for use in targeted therapies. The result of the cytotoxicity measurements demonstrates that, while NE3TA and NE3TA-Bn were substituted with a nitro group without compromising their cytotoxic activities (*C*-NE3TA and *N*-NE3TA, respectively), introduction of a nitro group into NETA backbone resulted in significantly decreased antiproliferative activity of NETA (*C*-NETA). Fluorescent cellular uptake study of C-NE3TA-NBD indicates that C-NE3TA is taken up into HT29 cancer cells. Both the nonfunctionalized chelators (NETA, NE3TA, and NE3TA-Bn) and the bifunctional chelators (*C*-NE3TA and *N*-NE3TA) possess great promise as cancer therapeutics. The two potent bifunctional ligands *C*-NE3TA and *N*-NE3TA can be linked to many peptides and monoclonal antibodies targeting to various types of tumor cells to generate the antitumor conjugates for use in targeted iron depletion therapy (IDT), which has been little explored.

Experimental Section

General. ^1H, ^{13}C, and NMR spectra were obtained using a Bruker 300 instrument and chemical shifts are reported in ppm on the δ scale relative to TMS, TSP, or solvent. Elemental microanalyses were performed by Galbraith Laboratories, Knoxville, TN. All reagents were purchased from Aldrich and used as received unless otherwise noted. Fast atom bombardment (FAB) high resolution mass spectra (HRMS) were obtained on JEOL double sector JMS-AX505HA mass spectrometer (University of Notre Dame, IN). The analytical HPLC was performed on an Agilent 1200 equipped with a dioarray detector (λ = 254 and 280 nm), with the themostat set at 35 °C and with a Zorbax Eclipse XDB-C18 column (4.6 × 150 mm, 80 Å). The mobile phase of a binary gradient (0–100% B/30 min; solvent A = 0.05 M AcOH/Et_3N, pH 6.0; solvent B = CH_3CN) at a flow rate of 1 mL/min was used for method 1. A combination of a binary gradient and an isocratic mobile phase (50–100% B/15 min; solvent A = H_2O; solvent B = CH_3CN and 100% B/15min) at a flow rate of 1 mL/min was used for method 2. Fluorescence spectra were recorded on a PC1 Photon counting spectrofluorometer (ISS, Inc., Champaign, IL) with excitation at 446 nm and bandwidth

of 8 nm. Flurorescence images were obtained using Olympus DSU spinning disk confocal microscope (Olympus America Inc., Melville, NY) with a band-pass filter set at 436/20nm (excitation) and 535/30 nm (emission). All UV absorbance measurements were obtained on an Agilent 8453 diode array spectrophotometer equipped with a eight-cell transport system (designed for 1 cm cells).

2-(Benzylideneamino)ethanol (1). To a solution of ethanolamine (1.23 g, 20.1 mmol) in anhydrous MeOH (50 mL) at 0 °C was added benzaldehyde (2.13 g, 20.0 mmol) and molecular sieves (10 pieces). The resulting mixture was gradually warmed to room temperature and stirred for 120 h. The reaction mixture was filtered while being rinsed with CH_2Cl_2. The filtrate was evaporated, and the residue was dried under vacuum overnight to afford an off-white oily compound **1** (2.63 g, 87%). The compound was used for the next step without further purification. ^{1}H NMR ($CDCl_3$) δ 2.40 (s, 1H), 3.70–3.80 (m, 2H), 3.85–4.00 (m, 2H), 7.35–7.50 (m, 3H), 7.68–7.79 (m, 2H), 8.32 (s, 1H); 8.11 (d, 2H); ^{13}C NMR ($CDCl_3$) δ 62.4, 63.2, 128.1, 128.5, 130.8, 135.7, 163.1.

2-(Benzylamino)ethanol (2). To a solution of **1** (2.62 g, 17.3 mmol) in anhydrous EtOH (55 mL) was portionwise added $NaBH_4$ (0.67 g, 17.7mmol) at 0 °C over 1 h. The resulting mixture was gradually warmed to room temperature and stirred for 20 h. The resulting mixture was filtered, and the filtrate was evaporated. The residue was dissolved in CH_2Cl_2 (50 mL) and filtered, and the filtrate was concentrated and dried in vacuo to afford **2** (1.86 g, 61%). ^{1}H NMR ($CDCl_3$) δ 2.60–2.70 (m, 2H), 3.60–3.73 (m, 2H), 7.24–7.27 (m, 5H); ^{13}C NMR ($CDCl_3$) δ 50.6, 53.4, 60.5, 126.9, 128.1, 128.4, 139.7. HRMS (Positive ion FAB) calcd for $C_9H_{13}NO$ $[M + H]^+$ *m/z*, 152.2163; found, 152.1075. The ^{1}H and ^{13}C NMR spectra of **3** are essentially identical to data reported previously.[28]

4-Benzyl-morpholin-2-one (3). To a mixture of **2** (356 mg, 2.4 mmol) and K_2CO_3 (565 mg, 4.1 mmol) in anhydrous CH_3CN (12 mL) at 0 °C was dropwise added benzyl-2-bromoacetate (540 mg, 2.4 mmol) over 0.5 h. The reaction mixture was gradually warmed to room temperature and stirred for 24 h. The resulting reaction mixture was filtered while washing with CH_2Cl_2, and the filtrate was concentrated to give **3**. ^{1}H NMR ($CDCl_3$) δ 2.70 (t, 2H), 3.30 (s, 2H), 3.60 (s, 2H), 4.40 (t, 2H), 7.20–7.40 (m, 5H); ^{13}C NMR ($CDCl_3$) δ 48.5, 55.6, 61.6, 68.7, 127.7, 128.5, 128.9, 136.0, 167.4. HRMS (positive ion FAB) calcd for $C_{11}H_{13}NO_2$ $[M + H]^+$ *m/z*, 192.0900; found, 192.1032.

***tert*-Butyl 2-(benzyl (2-hydroxyethyl) amino) Acetate (4).** To a solution of **2** (1.86 g, 12.3 mmol) and potassium carbonate (1.70 g, 12.3 mmol) in CH_3CN anhydrous (50 mL) at 0 °C was dropwise added *t*-butyl-bromoacetate (2.41 g, 12.4 mmol) over 45 min. The reaction mixture was gradually warmed to room temperature and stirred for 66 h. The resulting reaction mixture was filtered, and the filtrate was concentrated. The residue was then dissolved in CH_2Cl_2 (50 mL), the resulting solution was filtered, and the filtrate was concentrated to afford white compound **4** (2.94 g, 90%). ^{1}H NMR ($CDCl_3$) δ 1.45 (s, 9H), 2.86 (t, 2H), 3.23 (s, 2H), 3.54–3.62(m, 2H), 3.82 (s, 2H), 7.23–7.34 (m, 5H); ^{13}C NMR ($CDCl_3$) δ 28.0, 55.3, 26.5, 58.5, 58.8, 81.3, 127.3, 128.4, 128.8, 138.3, 171.0. HRMS (positive ion FAB) calcd for $C_{15}H_{24}NO_3$ $[M + H]^+$ *m/z*, 266.3605; found, 266.1756.

***tert*-Butyl 2-(benzyl (2-bromoethyl) amino) Acetate (5).** To a solution of **4** (2.94 g, 11.1 mmol) in anhydrous CH_2Cl_2 (40 mL) at 0 °C was added PPh_3 (3.49 g, 13.3 mmol). NBS (2.37 g, 13.3 mmol) was added portionwise into the reaction mixture over 1 h. The resulting mixture was stirred at 0 °C for 30 min, after which the ice bath was removed and the reaction mixture was stirred for 3 h. The resulting mixture was evaporated into a yellowish solid. The residue was dissolved in ether (100 mL). The solution was filtered, and the filtrate was evaporated and washed with ether again (3 × 50 mL). The filtrate was evaporated to give a white solid. The residue was then dissolved in ether (100 mL) and was passed through a short silica gel column to eliminate as much of triphenylphospine oxide as possible. The fractions containing the desired product were collected and dried. The residue was purified using column chromatography (silica gel, 60 mesh) eluted with 5% EtOAc in hexanes to provide **5** (1.83 g, 50%). ^{1}H NMR ($CDCl_3$) δ 1.47 (s, 9H), 3.10–3.18 (m, 2H), 3.31 (s, 2H), 3.30–3.40 (m, 2H), 3.88 (s, 2H), 7.20–7.38 (m, 5H); ^{13}C NMR ($CDCl_3$) δ 28.1, 30.5, 55.1, 55.9, 58.0, 81.0, 127.2, 128.3, 128.7, 138.7, 170.5. HRMS (positive ion FAB) calcd for $C_{15}H_{23}N_4O_2Br$ $[M + H]^+$ *m/z*, 328.0929; found, 328.0912.

4-[2-(Benzyl-*tert*-butoxycarbonylmethyl-amino)-ethyl]-7-*tert*-butoxycarbonyl-methyl-[1,4,7]triazonan-1-yl)-acetic Acid *tert*-Butyl Ester (7). To a solution of **6** (0.74 g, 2.1 mmol) in CH_3CN (60 mL) was added DIPEA (0.91 g, 7.1 mmol) and **5** (0.88 g, 2.8 mmol). The reaction mixture was stirred under reflux for 72 h after which the resulting solution was evaporated into a bright yellow residue (1.49 g). This residue was purified via column chromatography (silica gel, 60 mesh), eluting with 3% of methanol in dichloromethane to provide **7** as a yellowish solid (0.88 g, 71%). ^{1}H NMR ($CDCl_3$) δ 1.41 (d, 27H), 2.80–3.80 (m, 24H), 7.26–7.29 (m, 5H); ^{13}C NMR ($CDCl_3$) δ 28.0, 49.1, 49.3, 52.6, 53.7, 55.3, 57.7, 58.3, 81.5, 81.6, 127.6, 128.5, 129.1, 137.5, 170.3, 170.4. HRMS (positive ion FAB) calcd for $C_{33}H_{57}N_4O_6$ $[M + H]^+$ *m/z*, 605.8388; found, 605.4278. Analytical HPLC (t_R = 3.6 min, method 2).

(4-[2-Benzyl-carboxymethyl-amino)-ethyl]-7-carboxymethyl-[1,4,7]triazonan-1-yl) Acetic Acid (8). To a solution of **7** (0.09 g, 0.2 mmol) in 1,4-dioxane (5 mL) in an ice bath was added 4 M HCl in 1,4-dioxane (3 mL). The resulting mixture was gradually warmed to room temperature and stirred for 18 h. Ether (15 mL) was added to the reaction mixture, and the resulting mixture was stirred for 30 min. The resulting mixture was placed in the freezer for 2 h, and the solid residue was quickly filtered, washed with ether (10 mL), and dissolved in deionized water (18 MΩ). Evaporation of the aqueous solution provided an off-white solid **8** (0.07 g, 80%). ^{1}H NMR (D_2O) δ 2.93–3.03 (m, 4H), 3.15–3.22 (m, 6H), 3.32 (s, 4H), 3.40–3.50 (m, 2H), 3.90 (s, 4H), 3.97 (s, 2H), 4.35 (s, 2H), 7.20 to 7.40 (m, 5H); ^{13}C NMR (D_2O) δ 48.8, 49.8, 50.0, 50.2, 51.2, 53.7, 56.4, 59.6, 127.9, 129.5, 130.7, 131.4, 168.1, 170.4. HRMS (positive ion FAB) calcd for $C_{21}H_{33}N_4O_6$ $[M + H]^+$ *m/z*, 437.5162; found, 437.2400.

(4-Carboxymethyl-7-[2-(carboxymethyl-amino)-ethyl]-[1,4,7]-trizonan-1-yl) Acetic Acid (9). To a solution of 2 (100 mg, 0.20 mmol) in MeOH (10 mL) was added 10% wet Pd/C catalyst (30 mg). The resulting mixture was subjected to hydrogenolysis by agitation with excess H_2 (g) at 60 psi in a Parr hydrogenator apparatus at ambient temperature for 60 h. The reaction mixture was filtered through celite, and the filtrate was concentrated in vacuo under debenzylation apparatus for 60 h. The resulting mixture was filtered via celite bed and washed thoroughly with MeOH and water. The filtrate was evaporated to provide **9** as a yellowish solid (80 mg, 95%). ^{1}H NMR (D_2O) δ 3.10–3.18 (m, 4H), 3.28–3.35 (m, 12H), 3.58–3.63 (m, 2H), 3.88–3.94 (m, 6H); ^{13}C NMR (D_2O) δ 43.8, 43.9, 47.6, 48.8, 49.0, 49.2, 49.4, 50.1, 50.5, 50.7, 51.1, 51.9, 52.0, 53.0, 55.8, 56.3, 168.7, 171.4, 171.7. HRMS (positive ion FAB) calcd for $C_{20}H_{30}N_6O_9$ $[M + H]^+$ *m/z*, 347.1931; found, 347.1964.

2-(4-Nitrobenzylamino)ethanol (10). To a solution of ethanolamine (1.22 g, 20.0 mmol) in anhydrous MeOH (50 mL) at 0 °C was added 4-nitrobenzaldehyde (3.02 g, 20.0 mmol) and molecular sieves (10 pieces). The resulting mixture was gradually warmed to room temperature and stirred for 120 h. The reaction mixture was filtered while being rinsed with CH_2Cl_2. The filtrate was evaporated, and the residue was dried under vacuum overnight to afford yellowish oily imine compound (2.62 g, 87%). The compound was used for the next step without further purification. ^{1}H NMR ($CDCl_3$) δ 2.17 (s, 1H), 3.82 to 3.86 (m, 2H), 3.94 to 3.99 (m, 2H), 7.90–7.93 (d, 2H), 8.26 (d, 2H); ^{13}C NMR ($CDCl_3$) δ 61.8, 63.5, 123.8, 124.3, 128.8, 130.5, 141.2, 148.9, 160.9.

To a solution of the obtained imine compound (1.96 g, 10.0 mmol) in anhydrous EtOH (30 mL) was portionwise added $NaBH_4$ (0.38 g, 10.0 mmol) at 0 °C over 1 h period. The resulting mixture was gradually warmed to room temperature and stirred for 48 h. The resulting mixture was filtered, and the filtrate was evaporated. The residue was dissolved in CH_2Cl_2 (50 mL) and filtered, and the filtrate was concentrated in vacuo to afford **10** (1.86 g, 61%). ^{1}H

NMR ($CDCl_3$) δ 2.71 (t, 2H), 3.61 (t, 2H), 3.84 (s, 2H), 7.42 (d, 2H), 8.05 (d, 2H); ^{13}C NMR ($CDCl_3$) δ 50.7, 52.7, 60.9, 123.6, 128.7, 146.9, 147.8. The ^{1}H and ^{13}C NMR spectra of **10** are essentially identical to data reported previously.[30]

***tert*-Butyl [(2-Hydroxy-ethyl)-(4-nitro-benzyl)-amino] Ester (11).** To a solution of **10** (1.78 g, 9.0 mmol) and potassium carbonate (1.24 g, 9.0 mmol) in CH_3CN anhydrous (50 mL) at 0 °C was dropwise added *t*-butyl-bromoacetate (1.78 g, 9.0 mmol) over 1 h. The reaction mixture was gradually warmed to room temperature and stirred for 21 h. The resulting reaction mixture was filtered, and the filtrate was concentrated to give a yellowish oily compound. The residue was then dissolved in CH_2Cl_2 (50 mL), the resulting solution was filtered, and the filtrate was concentrated and dried in vacuo to afford yellowish oily compound **11** (2.94 g, 90%). ^{1}H NMR ($CDCl_3$) δ 1.44 (s, 9H), 2.83 (t, 2H), 3.23 (s, 2H), 3.59 (t, 2H), 3.91 (s, 2H), 7.51 (d, 2H), 8.15 (d, 2H); ^{13}C NMR ($CDCl_3$) δ 28.0, 55.7, 56.9, 58.7, 59.3, 81.7, 123.6, 129.3, 146.1, 147.2, 171.1. HRMS (positive ion FAB) calcd for $C_{15}H_{22}N_2O_5$ $[M + H]^+$ *m/z*, 311.1594; found, 311.1607.

***tert*-Butyl [(2-Bromo-ethyl)-(4-nitro-benzyl)-amino] Ester (12).** To a solution of **11** (1.87 g, 6.0 mmol) in anhydrous dichloromethane (40 mL) at 0 °C was added triphenylphosphine (1.90 g, 7.3 mmol). NBS (1.29 g, 7.3 mmol) was added portionwise into the reaction mixture over 1 h. The resulting mixture was stirred at 0 °C for 30 min, after which the ice bath was removed, and the reaction mixture was stirred for 3 h. The solvent was evaporated, and the residue was dissolved in ether (100 mL). The solution was filtered, and the filtrate was evaporated and washed with ether (3 × 100 mL). The filtrate was evaporated to give an oily compound that was then dissolved in ether (100 mL) and passed through a short silica gel column to eliminate triphenylphosphine oxide. The fractions containing the desired product were collected and concentrated in vacuo. Further purification was performed using column chromatography eluted with 20% EtOAc in hexane to afford compound **12** (1.83 g, 50%). ^{1}H NMR ($CDCl_3$) δ 1.44 (s, 9H), 3.12–3.15 (m, 2H), 3.30 (s, 2H), 3.30–3.40 (m, 2H), 3.98 (s, 2H), 7.54 (d, 2H), 8.14 (d, 2H); ^{13}C NMR ($CDCl_3$) δ 28.2, 30.4, 55.1, 55.8, 57.5, 81.6, 123.7, 129.2, 147.0, 147.3, 170.2. HRMS (positive ion FAB) calcd for $C_{15}H_{22}N_2O_4Br$ $[M + H]^+$ *m/z*, 373.0763; found, 373.0789.

***tert*-Butyl (4-*tert*-Butoxycarbonylmethyl-7-{2-[*tert*-butoxycarbonylmethyl-(4-nitro-benzyl)-amino]-ethyl}-[1,4,7]triazonan-1-yl) Ester (13).** To a solution of **6** (200 mg, 0.6 mmol) in CH_3CN (5 mL) was added DIPEA (217 mg, 1.8 mmol) and **12** (219 mg, 0.6 mmol). The reaction mixture was refluxed for 6 days. The resulting solution was evaporated into a yellow reddish residue. This residue is purified via column chromatography (silica gel, 220 mesh), eluting with 3% methanol in dichloromethane to afford a yellow oily compound **13** (88 mg, 24%). ^{1}H NMR ($CDCl_3$) δ 1.41 (d, 27H), 2.80–3.75 (m, 24H), 7.26 (d, 2H), 8.19 (d, 2H); ^{13}C NMR ($CDCl_3$) δ 28.2, 49.3, 49.9, 52.7, 53.6, 55.1, 57.4, 57.4, 81.8, 81.6, 123.6, 129.6, 145.8, 147.4, 170.0, 170.6. HRMS (positive ion FAB) calcd for $C_{33}H_{56}N_5O_8$ $[M + H]^+$ *m/z*, 650.4129; found, 650.4100. Analytical HPLC (t_R = 25 min, method 1).

(4-Carboxymethyl-7-{2-[carboxymethyl-(4-nitro-benzyl)-amino]-ethyl}-1,4,7]triazonan-1-yl)-acetic Acid (14). To a solution of **5** (13 mg, 0.1 mmol) in an ice bath was added 4 M HCl in 1,4-dioxane (5 mL). After the addition, the ice bath was taken out and the reaction mixture was gradually increased to room temperature and stirred for 18 h To this solution, ether (~15 mL) was added and was continuously stirred for 30 min. The resulting mixture was placed in the freezer for 2 h. Solid residue from recrystallization was quickly filtered and washed with ethyl ether (~50 mL), immediately dissolved in water, and lyophilized to provide pure **14** as a yellow solid (7 mg, 80%). ^{1}H NMR (D_2O) δ 2.82–2.85 (m, 4H), 2.94–2.96 (m, 2H), 3.12–3.14 (m, 4H), 3.28 (s, 4H) 3.38–3.40 (m, 2H), 3.81 (s, 6H), 4.50 (s, 2H), 7.70 (2, 2H), 8.22 (d, 2H); ^{13}C NMR (D_2O) δ 48.4, 48.8, 49.5, 50.4, 51.0, 52.0, 55.0, 56.4, 58.2, 124.3, 132.6, 135.9, 148.7, 169.6, 171.5. HRMS (positive ion FAB) calcd for $C_{21}H_{31}N_5O_8$ $[M + H]^+$ *m/z*, 481.2173; found, 481.2170.

***tert*-Butyl (4-*tert*-Butoxycarbonylmethyl-7-{2-(*tert*-butoxycarbonylmethyl-amino)-3-[4-(7-nitro-benzo[1,2,5]oxadiazol-4-ylamino)-phenyl]-propyl}-[1,4,7]triazonan-1-yl)-acetate (16).** To a solution of **15**[27b] (94 mg, 0.2 mmol) in CH_2Cl_2 (2 mL) was portionwise added NBD-Cl (30 mg, 0.2 mmol). The resulting mixture was stirred for 24 h while being protected from light by wrapping up the reaction apparatus using aluminum foil. The progress of the reaction was monitored by TLC analysis. The resulting solution was evaporated and purified via column chromatography (silica gel, 220 mesh), eluting with 1% methanol in CH_2Cl_2. The fractions containing **16** were collected and evaporated to provide **16** (31 mg, 26%). ^{1}H NMR ($CDCl_3$) δ 1.41–1.49 (m, 27H), 2.65–2.92 (m, 16H), 3.25–3.42 (m, 6H), 3.62–3.67 (m, 1H), 6.64 (d, 1H), 7.23–7.38 (m, 4H), 8.42 (d, 1H). HRMS (positive ion FAB) calcd for $C_{39}H_{58}N_8O_9$ $[M + H]^+$ *m/z*, 783.4405; found, 783.4434.

(4-Carboxymethyl-7-{2-(carboxymethyl-amino)-3-[4-(7-nitro-benzo[1,2,5]oxadiazol-4-ylamino)-phenyl]-propyl}-[1,4,7]triazonan-1-yl)acetic Acid (17). To a solution of **16** (16 mg, 0.1 mmol) in 1,4-dioxane (1 mL) at 0–5 °C was added 4 M HCl (g) in 1,4-dioxane (1 mL) dropwise over 15 min. The resulting mixture was allowed to warm to room temperature and stirred overnight. Ether (~15 mL) was added to the reaction mixture and stirred for 10 min. The resulting mixture was placed in the freezer for 1 h. The solid residue was filtered and washed with ether and quickly dissolved in deionized water (18 $\mu\Omega$). Evaporation of the aqueous solution provided pure **17** (12 mg, 90%) as an orange solid. ^{1}H NMR (CD_3OD) δ 2.82–3.48 (m, 13H), 3.78–4.08 (m, 10H), 6.76 (d, 1H), 7.40–7.55 (m, 4H), 8.51 (d, 1H). HRMS (positive ion FAB) calcd for $C_{27}H_{34}N_8O_9$ $[M + H]^+$ *m/z*, 615.2527; found, 615.2520.

Cell Culture. Human cervix HeLa cell line was obtained from ATCC (Rockville, MD) and cultured in minimum essential medium (MEM) with L-glutamine (2 mM), Earle's BSS, and sodium bicarbonate (1.5 g/L), supplemented with 10% fetal bovine serum (FBS), nonessential amino acids (0.1 mM), sodium pyruvate (1 mM), and antibiotic/antimycotic solution in a humidified atmosphere with 5% CO_2 at 37 °C. Human colon cancer cell line HT29 was kindly provided by professor Rajendra Metha (Illinois Institute of Technology Research Institute, Chicago, IL) and maintained in a humidified atmosphere with 5% CO_2 at 37 °C in RPMI-1640 medium, containing 10% FBS with L-glutamine and antibiotic/antimycotic. Lung fibroblast MRC-5 cell line was obtained from ATCC (Rockville, MD) and cultured in ATCC formulated EMEM, supplemented with 10% fetal bovine serum (FBS) in a humidified atmosphere with 5% CO_2 at 37 °C.

Antiproliferative Activity. Cells were seeded onto a 96-well plate at a density of 2000 cells for HeLa cells, 5000 cells for HT29 cells, or 5000 cells for MRC-5 per well in 0.1 mL complete medium and allowed to attach for 24 h. Varying concentrations of the test compounds in the final volume of 0.1 mL complete medium were then added in at least five series dilutions and incubated for 72 h. To measure cell proliferation, the Cell Titer 96 aqueous nonreactive cell proliferation assay (Promega Life Sciences, Madison, WI) was used according to the manufacturer's instructions. Briefly, MTS (2 mg/mL) and PMS (0.92 mg/ml) were mixed in a ratio of 20:1. An aliquot (20 μL) of the MTS/PMS mixture was added into each well, and the plate was incubated for 3 h at 37 °C. Optical absorbance at 490 nm was then recorded with an enzyme-linked immunosorbent assay (ELISA) microtiter plate reader (Biotek). Each experiment was done at least in triplicate. Antiproliferative activity of the test compounds was expressed as the fraction of optical densities of treated cells relative to the untreated solvent controls.[31] The data were plotted in GraphPad Prizm 3.0. Nonlinear regression analysis was used to determine IC_{50} values. IC_{50} values of the compounds were expressed as the concentration of the drugs inhibiting cell growth by 50%.

Iron Saturation Experiment. HeLa cells were inoculated onto 96-well plates at a density of 2000 per well in 0.1 mL complete medium and incubated for 24 h. The aqueous solution (50 μM) of the chelators, NETA, DFO, or DTPA was prepared and mixed with stoichiometric amount of aqueous solution (50 μM) of ferric citrate in complete medium, and the resulting mixture was then added into

the triplicate plates. Control samples containing no ferric citrate were also tested. Plates were incubated at 37 °C in 5% CO_2/95% air for 72 h. After the incubation, cells proliferation rates were evaluated by MTS assay.[31]

Fluorescence and UV Spectra of C-NE3TA-NBD. Fluorescence spectra were recorded on a PC1 photon counting spectrofluorometer (ISS, Inc., Champaign, IL) with excitation at 446 nm, bandwidth of 8 nm, data collection every 1 nm at 20 °C. Stock solution (1 mM) of NBD-NE3TA was prepared by dissolving sample in H_2O. UV–vis measurements were carried out by adding 20 μL aliquots of the stock solution via a micropipette into 2 mL of H_2O in a quartz cuvette, while the measurement of fluorescence was carried out by adding 1 μL aliquots of the stock solutions into 1 mL of H_2O in a quartz cuvette. The mixtures were stirred briefly for equilibration prior to data acquisition.

Flurorescence Imaging of Live Cancer Cells. HT29 cancer cells were plated in glass coverslips, which were placed in six-well plates and were incubated with growth media in a humidified atmosphere with 5% CO_2 at 37 °C overnight. Control cells or cells containing C-NE3TA-NBD (50 μM, H_2O) were incubated with media for 0.5 h under 5% CO_2 at 37 °C. At the end of the incubation time, cells were rinsed with PBS three times and subsequently observed under the Olympus DSU spinning disk confocal microscope with a band-pass filter set at 436/20nm (excitation) and 535/30 nm (emission).

Acknowledgment. The authors thank Dr. Nick Menhart for the flurorescence spectroscopy and Dr. Vytas Bindokas for the assistance in obtaining the fluoresence images.

References

(1) Buss, J. L.; Torti, F. M.; Torti, S. V. The role of iron chelation in cancer therapy. *Curr. Med. Chem.* **2003**, *10*, 1021–1034.
(2) Halliwell, B.; Gutteridge, J. M. *Free radicals in biological and medicine*; Claredon Press: Oxford, 1989.
(3) Kalinowski, D. S.; Richardson, D. R. The evolution of iron chelators for the treatment of iron overload disease and cancer. *Pharmacol. Rev.* **2005**, *57*, 547–583.
(4) Stevens, R. G.; Jones, D. Y.; Micozzi, M. S.; Taylor, P. R. Body iron stores and the risk of cancer. *N. Engl. J. Med.* **1988**, *319*, 1047–1052.
(5) Siegers, C. P.; Bumann, D.; Trepkau, H. D.; Schadwinkel, B.; Baretton, G. Influence of dietary iron overload on cell proliferation and intestinal tumorgenesis in mice. *Cancer Lett.* **1992**, *62*, 245–9.
(6) Buss, J. L.; Torti, F. M.; Torti, S. V. The role of iron chelation in cancer therapy. *Curr. Med. Chem.* **2003**, *10*, 1021–34.
(7) Huang, X. Iron overload and its association with cancer risk in humans: Evidence for iron as a carcinogenic metal. *Mutat. Res.* **2003**, *533*, 153–171.
(8) Faulk, W. P.; HsiI, B. L.; Stevens, P. J. Transferrin and transferring receptors in carcinoma of the breast. *Lancet* **1980**, *2*, 390–2.
(9) Keer, H. N.; Kozlowski, J. M.; Tsai, Y. C.; Lee, C.; McEwan, R. N.; Grayhack, J. T. Elevated transferrin receptor content in human prostate cancer cell lines assessed in vitro and in vivo. *J. Urol.* **1990**, *143*, 381–5.
(10) Kucharzewski, M.; Braziewicz, J.; Majewska, U.; Gozdz, S. Iron concentrations in intestinal cancer and in colon and rectum polyps. *Biol. Trace Elem. Res.* **2003**, *95*, 19–28.
(11) Brookes, M. J.; Hughes, S.; Turner, F. E.; Reynolds, G.; Sharma, N.; Ismail, T.; Berx, G.; McKie, A. T.; Hotchin, N.; Anderson, G. J.; Iqbal, T.; Tselepis, C. Modulation of iron transport proteins in human colorectal carcinogenesis. *Gut* **2006**, *55*, 1449–60.
(12) Chong, H. S.; Brechbiel, M. W. Synthesis of 1,3,5-*cis*,*cis*-triaminocyclohexane *N*-pyridyl derivatives as potential antitumor agents. *J. Org. Chem.* **2002**, *67*, 8072–8.
(13) Chong, H. S.; Torti, F. M.; Torti, S. Z.; Brechbiel, M. W. Synthesis and potent antitumor activities of novel 1,3,5-*cis*,*cis*-triaminocyclohexane *N*-pyridyl derivatives. *J. Med. Chem.* **2004**, *47*, 5230–4.
(14) Birch, N.; Wang, X.; Chong, H. S. Iron chelators as therapeutic iron depletion agents. *Expert Opin. Ther. Pat.* **2006**, *16*, 1533–57.
(15) Alvero, A. B.; Chen, W.; Sartorelli, A. C.; Schwartz, P.; Rutherford, T.; Mor, G. Triapine (3-aminopyridine-2-carboxaldehyde thiosemicarbazone) induces apoptosis in ovarian cancer cells. *J. Soc. Gynecol. Invest.* **2006**, *13*, 145–152.
(16) Krishna, G.; Mao, J.; Almassian, B.; Lang, W. Development of a parenteral formulation of an investigational anticancer drug, 3-aminopyridine-2-carboxaldehyde thiosemicar-bazone. *Pharm. Dev. Technol.* **1999**, *4*, 461.
(17) Le, N. T.; Richardson, D. R. Iron chelators with high antiproliferative activity up-regulate the expression of a growth inhibitory and metastasis suppressor gene: a link between iron metabolism and proliferation. *Blood* **2004**, *104*, 2967–75.
(18) Blatt, J.; Stitely, S. Antineuroblastoma activity of desferoxamine in human cell lines. *Cancer Res.* **1987**, *47*, 1749–50.
(19) Lederman, H. M.; Cohen, A.; Lee, J. W.; Freedman, M. H.; Gelfand, E. W. Deferoxamine: A reversible S-phase inhibitor of human lymphocyte proliferation. *Blood* **1984**, *64*, 748–53.
(20) Estrov, Z.; Tawa, A.; Wang, X. H; Dube, I. D.; Sulh, H.; Cohen, A.; Gelfand, E. W.; Freedman, M. H. In vitro and in vivo effects of deferoxamine in neonatal acute leukemia. *Blood* **1987**, *69*, 757–61.
(21) Dezza, L.; Cazzola, M.; Danova, M.; Carlo-Stella, C.; Bergamaschi, G.; Brugnatelli, S.; Invernizzi, R.; Mazzini, G.; Riccardi, A.; Ascari, E. Effects of desferrioxamine on normal and leukemic human hematopoietic cell growth: In vitro and in vivo studies. *Leukemia* **1989**, *3*, 104–7.
(22) Bridges, K. R.; Cudkowicz, A. Effect of iron chelators on the transferrin receptor in K562 cells. *J. Biol. Chem.* **1984**, *259*, 12970–7.
(23) Shen, L.; Zhao, H. Y.; Du, J.; Wang, F. Anti-tumor activities of four chelating agents against human neuroblastoma cells. *In Vivo* **2005**, *19*, 233–6.
(24) Brard, L; Granai, C. O.; Swamy, N. Iron chelators deferoxamine and diethylenetriamine pentacetic acid induce apoptosis in ovarian carcinoma. *Gynecol. Oncol.* **2006**, *100*, 116–27.
(25) Pippard, M. J.; Jackson, M. J.; Hoffman, K.; Petrou, M.; Modell, C. B. Iron chelation using subcutaneous infusions of diethylene triamine pentaacetic acid (DTPA). *Scand. J. Haematol.* **1986**, *36*, 466–72.
(26) Chong, H. S.; Garmestani, K.; Ma, D.; Milenic, D. E.; Overstreet, T.; Brechbiel, M. W. Synthesis and biological evaluation of novel macrocyclic ligands with pendent donor groups as potential yttrium chelators for radioimmunotherapy with improved complex formation kinetics. *J. Med. Chem.* **2002**, *45*, 3458–64.
(27) (a) Chong, H. S.; Ma, X.; Lee, T.; Kwamena, B.; Milenic, D. E.; Brady, E. D.; Song, H. A.; Brechbiel, M. W. Rational design and generation of a bimodal bifunctional ligand for antibody-targeted radiation cancer therapy. *J. Med. Chem.* **2008**, *51*, 118–125. (b) The synthesis and characterization of C-NETA and C-NE3TA analogues will be reported elsewhere.
(28) Huskens, J.; Sherry, A. D. Synthesis and characterization of 1,4,7-triazacyclononane derivatives with methylphosphinate and acetate side chains for monitoring free Mg^{II} by ^{31}P and ^{1}H NMR spectroscopy. *J. Am. Chem. Soc.* **1996**, *118*, 4396–4404.
(29) Richard, H.; Smith, Jr.; Wladkowski, B. D.; Taylor, J. E.; Thompson, E. J.; Pruski, B.; Klose, J. R.; Andrews, A. W.; Michejdat, C. J. Acid-catalyzed decomposition of 1-alkyltriazolines: A mechanistic study. *J. Org. Chem.* **1993**, *58*, 2097–2103.
(30) Kumpaty, H. J.; Bhattacharyya, S.; Rehr, E. W.; Gonzalez, A. M. Selective access to secondary amines by highly controlled reductive mono-N-alkylation of primary amines. *Synthesis* **2003**, *14*, 2201–10.
(31) Cory, A. H.; Owen, T. C.; Barltrop, J. A.; Cory, J. G. Use of an aqueous soluble tetrazolium/formazan assay for cell growth assays in culture. *Cancer Commun.* **1991**, *3*, 207–12.

JM701307J